agriculture

MDPI

Article

A Channel Attention-Driven Optimized CNN for Efficient Early Detection of Plant Diseases in Resource Constrained Environment

Sana Parez [1], Naqqash Dilshad [2] and Jong Weon Lee [1,*]

[1] Department of Software, Sejong University, Seoul 05006, Republic of Korea; parez.sana@gmail.com
[2] Department of Computer Science and Engineering, Sejong University, Seoul 05006, Republic of Korea; dilshad.naqqash@gmail.com or dilshad.naqqash@sejong.ac.kr
* Correspondence: jwlee@sejong.ac.kr

Abstract: Agriculture is a cornerstone of economic prosperity, but plant diseases can severely impact crop yield and quality. Identifying these diseases accurately is often difficult due to limited expert availability and ambiguous information. Early detection and automated diagnosis systems are crucial to mitigate these challenges. To address this, we propose a lightweight convolutional neural network (CNN) designed for resource-constrained devices termed as *LeafNet*. *LeafNet* draws inspiration from the block-wise VGG19 architecture but incorporates several optimizations, including a reduced number of parameters, smaller input size, and faster inference time while maintaining competitive accuracy. The proposed *LeafNet* leverages small, uniform convolutional filters to capture fine-grained details of plant disease features, with an increasing number of channels to enhance feature extraction. Additionally, it integrates channel attention mechanisms to prioritize disease-related features effectively. We evaluated the proposed method on four datasets: the benchmark plant village (PV), the data repository of leaf images (DRLIs), the newly curated plant composite (PC) dataset, and the BARI Sunflower (BARI-Sun) dataset, which includes diverse and challenging real-world images. The results show that the proposed performs comparably to state-of-the-art methods in terms of accuracy, false positive rate (FPR), model size, and runtime, highlighting its potential for real-world applications.

Keywords: plant disease classification; smart agriculture; precision farming; attention mechanism; VGG19

Academic Editor: Francesco Marinello

Received: 14 November 2024
Revised: 24 December 2024
Accepted: 7 January 2025
Published: 8 January 2025

Citation: Parez, S.; Dilshad, N.; Lee, J.W. A Channel Attention-Driven Optimized CNN for Efficient Early Detection of Plant Diseases in Resource Constrained Environment. *Agriculture* **2025**, *15*, 127. https://doi.org/10.3390/agriculture15020127

1. Introduction

In recent times, agriculture has become the main source of livelihood for many countries and plays a vital role in the global economy. According to the World Bank [1], agriculture employed over a billion people in 2018, accounting for 28.5% of the total workforce, and produced approximately 10 million tons of food daily. However, plant infections and diseases threaten the potential of agriculture, jeopardizing food security. Plant viruses may cause significant losses to major food crops such as wheat, rice, soybeans, maize and potatoes, which can range from 10% to 40% [2]. It could be ineffective and time-consuming to constantly examine illness signs in order to address these issues, especially in large crop fields. Precision agriculture hinges on the effective detection of plant infections. As a result, research groups have turned to ML to harness its potential for detecting plant diseases automatically using the analysis of field-acquired images. These researchers analyze these images to extract meaningful features. For instance, in a study by [3], the classification of guava leaf diseases was accomplished by applying a support vector machine (SVM) after picture characteristics were extracted using scale-invariant feature transform (SIFT).

In another approach, before using SVM, the authors of [4] used the gray level co-occurrence matrix (GLCM) rather than SIFT. Other research has analyzed plant diseases using a variety of feature extraction techniques, with notable results [5–8].

For intricate data designs and sizable training datasets, several researchers have opted to utilize the k-nearest neighbors (K-NN) classifier rather than kernel vector machines (SVM). For instance, local statistical input characteristics were employed to classify Cotton Grey Mildew illness using K-NN [9]. It has also been used to classify paddy leaves and groundnut leaf diseases [10,11]. However, all of these approaches require multiple steps for data preparation, pre-processing, and feature extraction. Furthermore, their efficacy in managing multi-class data categorization remains unproven, and they exhibit sensitivity to predetermined parameters like the kernel parameters 'k' in Support Vector Machines and 'f' in K-Nearest Neighbors [12]. Some researchers have resorted to deep learning (DL) approaches in order to overcome these problems and enhance the identification of agricultural illnesses and infections. A DL-based system named PV, for instance, was created by [13] and is capable of precisely identifying 26 distinct plant diseases. Unlike explicit feature extraction techniques, DL algorithms automatically recognize and extract relevant properties from input photographs. However, in order to classify 2D pictures into 1D vectors, conventional artificial neural network (ANN) classifiers lose spatial information, which raises the computing and storage needs. In another study, ref. [14] authors introduced a methodology for plant disease classification based on a novel dataset called DRLI.

Neural networks, particularly CNNs, have been shown to be very effective in addressing the limitations of deep neural networks (DNNs) in agriculture [15]. For instance, the MaskRCNN model with transfer learning was employed by [16] to detect fusarium head blight disease in wheat. On a test dataset of about 450 photos, their method yielded an average accuracy of 92.01%. A similar methodology was used by [17] to identify apple leaf diseases. They achieved recognition accuracies of 77.65%, 75.59%, and 73.50% using the ResNet152, Inception V3, and MobileNet models, respectively. Ref. [18] also developed a custom deep CNN using the PV dataset to classify cucumber infections. Their model achieved an impressive accuracy of up to 94% by leveraging a pre-trained AlexNet model. Another example is the development of a Custom-Net model by [19] utilizing Raspberry Pi (RPi) for the classification of pearl millet illnesses, with an astounding accuracy rate of 98.78%. DL models, which frequently make use of the PV dataset, have also been applied extensively to identify different leaf illnesses. These approaches have achieved high classification accuracy, especially when it comes to the infection of the tomato leaf (97.49% accuracy) [20], and banana leaf diseases (99.72% accuracy) [21].

To assist farmers in addressing issues, including water scarcity, nutritional imbalances, diseases, weeds, and pests, artificial intelligence (AI) models and machine learning (ML) approaches are being deployed on drones. Because they are long-range, reasonably priced, and AI-compatible, drones are widely used in precision agriculture [22]. Presently identified and emphasized research gaps are as follows:

- **IoT Environment Suitability:** Most existing models, including CNNs and attention mechanisms, are too resource-intensive for IoT devices, which have limited computational power and memory.
- **Computational and Memory Constraints:** Current models do not account for the severe limitations in computing resources, power, and memory capacity typical of IoT devices, making them impractical for deployment in such environments.
- **Need for Lightweight Models:** There is a clear need for developing lightweight models that can operate efficiently under the constraints of IoT devices. Present solutions fail to meet these requirements, limiting their real-world applicability.

To address these challenges and research gaps, our work has made the following significant contributions:

1. We have developed *LeafNet*, a lightweight DL model optimized for operation on resource-constrained devices (RCDs), effectively addressing the limited processing power of real-world IoT devices. By utilizing fewer parameters, *LeafNet*achieves higher accuracy compared to other lightweight networks such as EfficientNetB0, MobileNetV1, and MobileNetV3Small. Notably, *LeafNet* requires 3.29 million and 1.76 million fewer parameters than MobileNetV1 and MobileNetV3Small, respectively. This reduction enhances its computational efficiency, making it particularly well-suited for deployment on devices with restricted computational resources. To promote reproducibility and facilitate further research, the source code is publicly available at: (https://github.com/sanaparez/LeafNet) (accessed on 5 January 2024).
2. We evaluated our lightweight DL model using four plant disease detection datasets: PV, DRLI, our proprietary PC dataset, and BARI-Sun dataset. To benchmark its performance, we compared it against several state-of-the-art (SOTA) models, including VGG19 [23], VGG16 [23], EfficientNetB0 [24], MobileNetV1 [25], MobileNetV3Small [26], ResNet50 [27], ResNet152 [27], ViT-B/32 [28], MobileViT-S [29], and MobileOne-S0 [30]. *LeafNet* outperformed all these state-of-the-art models in terms of accuracy, false alarm rates (FARs), and computational efficiency, demonstrating its superior effectiveness for plant disease detection.
3. We integrated a Channel Attention (CA) module to refine and enhance intermediate feature extraction, which significantly improved the model's performance by fine-tuning the most relevant characteristics. By effectively extracting features, *LeafNet* is capable of directly categorizing input images into distinct groups without requiring intermediary processes. We conducted a comprehensive evaluation of *LeafNet*, considering factors such as computational requirements, model size, and training time. The results highlight the suitability of *LeafNet* for deployment on devices with limited computational resources, demonstrating its efficiency and practicality.

The parts below are further divisions of this paper: Section 2 contains the previous relevant material. The methodology, which outlines the essential procedures and methods used in this investigation, is provided in Section 3. A brief overview of the experimental results derived from the datasets contained is given in Section 4. The study concludes with Section 5, which summarizes the key results, contributions, and suggested courses of future research.

2. Related Works

With an emphasis on the several CNN models put out by various researchers, this section examines earlier efforts pertaining to the issue of classifying plant diseases. To detect illnesses in tomato, potato, and corn plants, ref. [31] presented a technique combining an inception module and residual connection. An online platform for the real-time detection of diseases was also proposed by them. By utilizing a dataset of 10,851 field photos, an attention-based dense CNN model was able to identify 44 distinct plant disease categories with 97.33% accuracy [32]. A CNN-based convolutional Auto-Encoder approach was presented by [33], which achieved 98.38% accuracy in classifying Bacterial Spot disease in peach plants. Ref. [34] suggested a modified version of the CNN model. In order to identify diseases in fifteen different plants. Ref. [35] introduced the InceptionResNet model with the aim of categorizing 15 distinct forms of plant diseases. Ref. [36] introduced the EfficientNet concept, and 39 different disorders were found in the PV dataset. Combining characteristics from the deep CNN models EfficientNetB01 and DenseNet121 allowed the authors to obtain 98.56% accuracy in diagnosing maize leaf diseases [37]. In another study,

the authors employed a Vision Transformer network that had been trained beforehand to identify diseases in the PV dataset [38].

The works that fall within the miscellaneous category and are suggested for plant disease classification by various researchers are outlined below: Generative adversarial networks were used by [39] to create artificial pictures of sick tomato plant leaves. Furthermore, they achieved a classification accuracy of 97.11% by applying the DenseNet121 model to classify five different types of potato plant illnesses. Using datasets from Apple, Maize, and Rice, ref. [40] achieved an average accuracy of over 93% in plant disease categorization using the vision transformer (ViT) architecture. A deep CNN technique with an attention mechanism was presented by [41] for the classification of tomato leaf disease. When tested on 24,001 photos, their model successfully identified 98% of the instances. In another study [42], the authors proposed DFN-PSAN, which incorporates YOLOv5 as a feature extractor and employs pyramidal squeezed attention (PSA) combined with multiple convolutional layers to design PSAN, which achieves an accuracy of 95.27% on the PV dataset. A teacher/student architecture for recognizing 14 distinct plant diseases was proposed by [43].

The majority of the previously described efforts rely on CNN architecture's convolution or attention methods. Unfortunately, due to memory and computing power limitations, these models are not appropriate for Internet of Things (IoT) scenarios. Limited processing power, memory, and resources are only a few of the issues that the IoT must deal with [44]. The suggested work offers a lightweight, non-convolutional, attention-mechanism method that solves these issues and is perfect for IoT implementation. The suggested model makes use of a multi-tier meta-ensemble technique, in which a second-level model is trained using characteristics derived from the prediction probabilities of first-level trained models. The suggested solution's classification performance is improved by using the meta-ensemble approach.

3. The Proposed Methodology

In this section, a technical explanation is provided for each module of the proposed model. The proposed *LeafNet* architecture is based on the modified VGG19 architecture, which has accuracies of Top-1 and Top-5 of 71.3% and 90.0% on the ImageNet benchmark dataset, respectively. Due to the robust performance architecture, we chose VGG19 and further modified the original architecture for the task at hand. In addition, channel attention has been coupled with the base feature extractor to further enhance the selection of optimal features. The proposed method is evaluated on four publicly available benchmark datasets. Further details are provided in the subsequent sections.

3.1. The LeafNet Architecture

CNNs are widely used for monitoring complex video surveillance tasks, including the identification of objects, categorization, anomaly detection, and activity and action recognition, as well as various applications in identification, medical image diagnosis, video summarization, and segmentation. The convolution layer (CL), the pooling layer, and the fully linked layer make up the three primary parts of the CNN design. A deep CNN consists of a single input layer and multiple hidden layers, fully connected layers, and softmax layers. To create feature maps from deep CNNs, parameters like local receptive fields and various kernels are used to highlight the important features of objects in the images. For dimensionality reduction, these feature maps are reduced through sub-sampling using average, minimum, or maximum pooling.

Choosing the right CNN architecture for a specific application is a complex task that involves balancing the need for good results with computational efficiency. Each CNN ar-

chitecture has its own set of strengths and weaknesses. The designs of VGG19 and AlexNet, for instance, are rather simple to design and implement. A standard in DL, AlexNet made its debut in the ImageNet competition. Performance is often thought to be improved by increasing the number of CL in a network, as the VGG model illustrates. Research suggests VGG19, a 19-layer architecture, as a reliable feature extractor that can handle big datasets and challenging backdrop identification tasks. In classification tasks, this design significantly outperforms the previous one while maintaining the same filter size.

In terms of total size and training parameters, VGG19 and VGG16 are not resource-efficient despite their many advantages. With EfficientNetB0 and MobileNetV1 especially built for quick inference times, these architectures as well as MobileNetV3Small, MobileViT-S, and MobileOne-S0 are far less expensive and more robust than others. This article suggests an effective plant disease detection and classification model termed as *LeafNet*, taking into account resource processing costs, real-world implementation, and the shortcomings of existing lightweight models. In Figure 1, the suggested framework is shown.

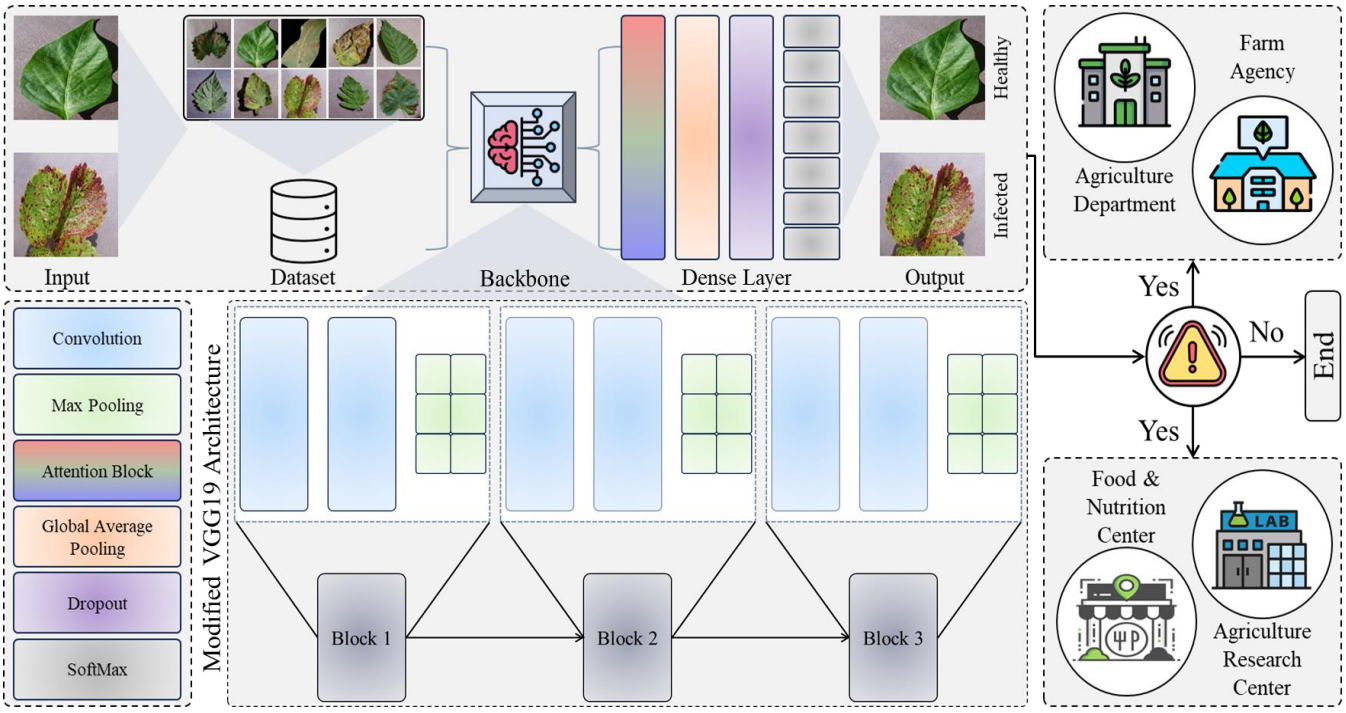

Figure 1. The proposed optimized *LeafNet* for efficient plant disease detection.

Initially, we evaluated the performances of prominent pre-trained CNN architectures, such as VGG19, VGG16, EfficientNetB0, MobileNetV1, MobileNetV3Small, ResNet50, ResNet152, ViT-B/32, MobileViT-S, and MobileOne-S0, before developing our new framework. This study particularly focuses on successfully extracting infected spots using visually perceptible data. To enhance the recognition of disease regions, we used a smaller version of the captured image, unlike previous CNNs. We also removed Block-4, Block-5, and Block-6 of VGG19 to reduce the number of parameters and training time. Despite having fewer parameters, the model achieved higher accuracy compared to other state-of-the-art models and offered a higher frame per second (FPS). Furthermore, the approach uses a smaller input size to capture minute details, allowing the classifier to learn more distinctive features.

With three channels and 32 different red, green, and blue (RGB) filters, the input picture size for the proposed model is 128 × 128. Deep feature extraction is achieved by progressively increasing the scale of each filter in each block. The filter sizes for the first,

second, and third blocks are set at 64, 128, and 256, respectively. Each layer of the proposed model applies a linear function called rectified linear activation (ReLU), which outputs a direct value if the input is positive and zero otherwise. The input from the third block is then passed to the pooling layers, where global average pooling (GAP) is applied before being forwarded to the Softmax layer. This layer categorizes the output into two classes: healthy and infected.

3.2. Channel Attention Mechanism

We use a channel attention module to re-calibrate the features in order to effectively choose the characteristics that substantially contribute to the final output. The channel attention module is comprised of two fully connected layers, a multiplication operation, and a global average pooling (GAP) operation, as seen in Figure 2.

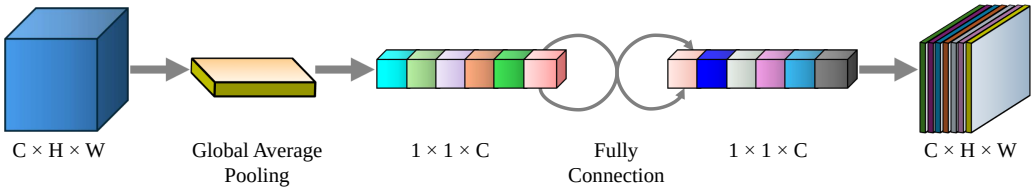

Figure 2. Two completely linked layers, a multiplication operation, and GAP make up the channel attention module. This module has the ability to re-calibrate the input feature maps.

For each i, j, and c in the c-th feature map, where $i \in [0, H-1]$, $j \in [0, W-1]$, and $c \in [0, C-1]$, let $u_c(i, j)$ represent the feature intensity (activation value) at spatial location (i, j) in the c-th channel of the input feature map. To compress the feature map u_c into a vector along the spatial dimension (of size $1 \times 1 \times C$), GAP is applied, which computes the average value of the spatial activations. The resulting vector captures the input feature maps' global receptive field and is defined as:

$$z_c = G(u_c) = \frac{1}{H \times W} \sum_{i=0}^{H-1} \sum_{j=0}^{W-1} u_c(i, j) \tag{1}$$

Here, z_c denotes the output vector for channel c, and $G(\cdot)$ represents the global average pooling operation. The vector z_c is then passed through two stacked fully connected layers to generate the learnable parameters.

The process of obtaining the learnable parameters s_c is illustrated in Equation (2):

$$s_c = \sigma(w_2 \otimes \delta(w_1 \otimes z_c)) \tag{2}$$

Here, w_1 and w_2 denote the weight matrices, δ represents the ReLU activation function, σ is the sigmoid activation function, and the convolution operation is denoted by the symbol "$\otimes$".

The re-calibration of the original features is achieved by applying channel-wise multiplication. Specifically, a weighted combination of the original features u_i and the learnable parameters s_c produces the final output feature for each channel. This process is expressed as:

$$x_{\text{out}} = s_i \cdot u_i, \quad \text{where } i \in [0, C-1]. \tag{3}$$

4. Experimental Results and Discussion

Measures and processes for assessments are covered in this section. We first describe the experimental design and key performance indicators, and then we go over the results of the assessment. To retain previously learned information, all models including

our suggested *LeafNet* were trained with a modest learning rate for a total of 10 epochs. For the purpose of maximizing performance on the intended dataset, the pre-trained model modified its parameters continually.

4.1. Implementation Details

The newly designed *LeafNet* model uses 128 × 128 and a batch size of 32, whereas each model was retrained using its default input size of 224 × 224 after receiving the first results. A 1×10^{-4} learning rate and 0.9 momentum were used for the Adam optimizer. This NVIDIA GeForce RTX 3090 GPU boasts 24 GB of on-chip memory and 64 GB of onboard memory, which was utilized in this study. This GPU achieves a maximum of 36 Tera FLOPS (Floating Point Operations Per Second). We utilized TensorFlow 2.9.1 in the backend and the Keras [45] DL framework for experiments. Several standard performance measures, such as accuracy, F1-score, precision, and recall, were used to assess the suggested *LeafNet* model.

4.2. Datasets

The study used PV and DRLI, two widely used standard datasets, to evaluate the efficacy of the suggested model. In addition, a new dataset named PC dataset, which was produced by combining the two datasets was used to evaluate the robustness of the theory. Although the detailed information is given below, the combined dataset details are shown in Table 1.

Table 1. Sample counts for healthy and infected categories in the employed datasets.

Dataset	Healthy	Infected	Total
PV	15,084	39,221	54,305
DRLI	2278	2225	4503
PC	17,361	41,446	58,807
BARI-Sun	515	1314	1829

1. **PV dataset** is a vast and intricate collection of data, encompassing 14 distinct plant species and comprising a total of 38 unique classes. Among these classes, twenty-six are dedicated to depicting infected plants, while the remaining 12 depict the healthy ones. In terms of sheer volume, this dataset boasts a substantial 54,305 images, with 15,084 representing the healthy plant classes and a substantial 39,221 showcasing the infected plant classes. It is worth noting that this diverse dataset contains images of various plant types, including tomatoes, strawberries, grapes, and oranges.
2. **DRLI dataset** is comprised of a dozen different plant types, i.e., jamun, basil, pomegranate, jatropha, lemon, astonia, arjun, bael, guava, mango, and scholaris. Researchers photographed the leaflets in both healthy and infected states, categorizing them as "healthy" or "infected". The dataset contains around 4503 images, with 2278 featuring healthy leaves and 2225 displaying diseased leaves. To facilitate the researchers, the dataset was divided into twenty-two subject groups, each corresponding to a specific plant species.
3. **PC dataset** The authors combined two publicly accessible datasets, PV and the DRLI, to perform an experiment to evaluate the robustness of the suggested *LeafNet* model. Because of this fusion, a new and more varied dataset was produced, which increased the model's problems. With 58,807 pictures in total, this composite dataset is 7.6% larger than PV and significantly larger than the DRLI dataset, i.e., 92.3%. The model needed to go through a rigorous training procedure because of the larger dataset and the inclusion of a greater range of plant species. As a result, the model demonstrated better generalization skills and increased dependability for situations involving the real-time identification of plant diseases, providing an invaluable visual aid.

4. **BARI-Sun dataset** was created using images collected from the demonstration farm of the Bangladesh Agricultural Research Institute (BARI) in Gazipur. This dataset initially consisted of 467 raw images, featuring both healthy sunflower leaves and flowers, as well as those affected by diseases [46]. To address the need for a larger dataset, which is essential for training DL models, data augmentation techniques were applied. Spatial augmentations included random rotation, scaling, cropping, shifting, as well as the addition of noise and blurring. For color enhancement, the brightness, contrast, saturation, and hue of images were adjusted. After augmentation, the dataset expanded to include 470 samples of Downy mildew, 509 samples of Leaf scars, 398 samples of Gray mold, and 515 samples of Fresh (healthy) leaves. All images were resized to 512 × 512 pixels and saved in JPG format.

4.3. Evaluation Metrics

A number of assessment criteria, including accuracy, precision, recall, and F1-score, were used to evaluate the suggested *LeafNet* model.

$$\text{Accuracy} = \left(\frac{\text{True Positive} + \text{False Negative}}{\text{True Positive} + \text{True Negative} + \text{False Positive} + \text{False Negative}} \right), \quad (4)$$

$$\text{Precision} = \left(\frac{\text{True Positive}}{\text{True Positive} + \text{False Positive}} \right), \quad (5)$$

$$\text{Recall} = \left(\frac{\text{True Positive}}{\text{True Positive} + \text{False Negative}} \right), \quad (6)$$

$$\text{F1-score} = 2 \times \left(\frac{\text{Precision} \times \text{Recall}}{\text{Precision} + \text{Recall}} \right). \quad (7)$$

4.4. Quantitative Results

In order to identify plant diseases, this study compared a number of pre-trained CNN-based designs with *LeafNet*. Accuracy, precision, recall, F1-score, and the number of trainable parameters were the main assessment criteria during the performance evaluation. The majority of the models under investigation, including ViT-B/32, EfficientNetB0, MobileNetV1, MobileNetV3Small, ResNet50, ResNet152, VGG19, VGG16, as well as MobileViT-S and MobileOne-S had comparable results. In contrast, the suggested *LeafNet* model demonstrated the lowest FAR when compared to the other state-of-the-art models and achieved superior accuracies of 99%, 98%, 99% and 0.96% on all four datasets. Nevertheless, the ViT-B/32 performed the worst when compared to the other models. Interestingly, the suggested *LeafNet* outperformed all of the available datasets and showed low FAR when compared to MobileNetV1, despite the fact that both models showed nearly the same computational efficiency. Tables 2 and 3 provide a thorough performance comparison of the models used. Clearly, the trained models work well with a little FAR. Still, there is room for improvement as the FAR is still high. Therefore, with an emphasis on accuracy and a reduction in false predictions, this study investigates the pre-training and optimization of a CNN architecture, namely *LeafNet*. With the most accurate detection among the other models, *LeafNet* performs the best after fine-tuning.

Table 2. Quantitative comparison of *LeafNet* with state-of-the-art models using the datasets provided. In blue, the suggested *LeafNet* model is emphasized. An upward arrow (⇑) indicates that a greater value is preferable.

Technique	Class	PV				DRLI				PC			
		P	R	F1	ACR ⇑	P	R	F1	ACR ⇑	P	R	F1	ACR ⇑
VGG19	Healthy	1.00	0.95	0.98	0.99	0.96	0.97	0.97	0.97	0.99	0.96	0.97	0.98
	Infected	0.98	1.00	0.99		0.97	0.96	0.96		0.98	1.00	0.99	
VGG16	Healthy	0.99	0.99	0.99	1.00	0.98	0.94	0.96	0.96	0.99	0.99	0.99	0.99
	Infected	1.00	1.00	1.00		0.93	0.98	0.96		0.98	1.00	1.00	
EfficientNetB0	Healthy	1.00	1.00	1.00	1.00	0.99	0.83	0.90	0.89	1.00	0.97	0.98	0.99
	Infected	1.00	1.00	1.00		0.78	0.98	0.87		0.99	1.00	0.99	
MobileNetV1	Healthy	1.00	0.99	0.99	1.00	0.97	0.96	0.97	0.97	0.99	0.99	0.99	0.99
	Infected	1.00	1.00	1.00		0.96	0.97	0.96		1.00	1.00	1.00	
MobileNetV3Small	Healthy	1.00	1.00	1.00	1.00	0.93	0.99	0.96	0.96	1.00	0.99	0.99	0.99
	Infected	1.00	1.00	1.00		0.99	0.93	0.95		0.99	1.00	1.00	
ResNet50	Healthy	1.00	1.00	1.00	1.00	0.93	0.99	0.96	0.96	1.00	0.99	0.99	0.99
	Infected	1.00	1.00	1.00		0.99	0.93	0.95		0.99	1.00	1.00	
ResNet152	Healthy	1.00	1.00	1.00	1.00	0.93	0.99	0.96	0.96	1.00	0.99	0.99	0.99
	Infected	1.00	1.00	1.00		0.99	0.93	0.95		0.99	1.00	1.00	
ViT-B/32	Healthy	0.92	0.98	0.95	0.95	0.81	0.62	0.70	0.75	0.87	0.95	0.91	0.94
	Infected	0.98	0.92	0.95		0.71	0.86	0.78		0.98	0.94	0.96	
MobileViT-S	Healthy	0.92	0.93	0.92	0.93	0.71	0.71	0.70	0.71	0.90	0.90	0.91	0.91
	Infected	0.93	0.92	0.92		0.70	0.70	0.71		0.91	0.90	0.90	
MobileOne-S0	Healthy	0.99	0.99	1.00	1.00	0.97	0.97	0.96	0.97	0.99	0.99	1.00	0.99
	Infected	1.00	0.99	0.99		0.96	0.97	0.97		0.99	1.00	0.99	
The proposed *LeafNet*	Healthy	1.00	0.97	0.98	0.99	0.97	1.00	0.98	0.98	0.99	0.98	0.99	0.99
	Infected	0.99	1.00	0.99		1.00	0.97	0.99		0.99	1.00	0.99	

Table 3. Quantitative comparison of *LeafNet* with state-of-the-art models using the BARI-Sun dataset. In blue, the suggested *LeafNet* model is emphasized. An upward arrow (⇑) indicates that a greater value is preferable.

Technique	Class	BARI-Sunflower			
		P	R	F1	ACR ⇑
VGG19	Healthy	0.96	0.95	0.94	0.95
	Infected	0.95	0.94	0.95	
VGG16	Healthy	0.94	0.94	0.95	0.94
	Infected	0.95	0.94	0.94	
EfficientNetB0	Healthy	0.86	0.89	0.88	0.88
	Infected	0.89	0.88	0.88	
MobileNetV1	Healthy	0.94	0.95	0.94	0.95
	Infected	0.95	0.94	0.95	
MobileNetV3Small	Healthy	0.96	0.95	0.94	0.95
	Infected	0.94	0.96	0.95	
ResNet50	Healthy	0.93	0.94	0.93	0.94
	Infected	0.94	0.95	0.94	
ResNet152	Healthy	0.95	0.94	0.95	0.95
	Infected	0.94	0.95	0.94	

Table 3. *Cont.*

Technique	Class	BARI-Sunflower			
		P	R	F1	ACR ⇑
ViT-B/32	Healthy Infected	0.73 0.72	0.72 0.72	0.72 0.73	0.72
MobileViT-S	Healthy Infected	0.68 0.67	0.69 0.70	0.69 0.69	0.69
MobileOne-S0	Healthy Infected	0.95 0.94	0.94 0.95	0.95 0.94	0.95
The proposed *LeafNet*	Healthy Infected	0.95 0.96	0.96 0.95	0.96 0.96	0.96

Figure 3 displays the confusion matrix of the *LeafNet* method, which was trained using the benchmark datasets provided. The green diagonal indicates true positives and true negatives, and the red displays misclassifications. Compared to the state-of-the-art models, the recommended *LeafNet* shows superior overall classification accuracy, despite some misclassifications within both categories. The accuracy and loss graphs for training are shown in Figure 4. Although there are occasional miss-classifications in each category, the proposed *LeafNet* outperforms the state-of-the-art models in terms of overall classification accuracy. Figure 4 shows the accuracy and loss graphs obtained during training. Accuracy and loss are displayed on the vertical axis, while the total number of epochs is displayed on the horizontal. To see how successfully *LeafNet* identifies plant diseases, see Figure 4. An increase in the number of training and validation cycles causes variations in the line graphs of training and validation accuracy, as shown in Figure 4a. For the PV, DRLI, PC and BARI-Sun datasets, respectively, the proposed *LeafNet* converges after seven epochs and yields 99%, 97%, 99% and 0.96% training and validation accuracies. Figure 4b illustrates how the training and validation loss values change and ultimately get closer to zero. A comparison of the suggested *LeafNet* with the other pre-trained models is also shown in Tables 2 and 3. The performance of the proposed *LeafNet* is better than the other pre-trained models, as evident from the extensive quantitative analysis of all four datasets against ten state-of-the-art models in Tables 2 and 3.

4.5. Qualitative Results

We performed a study to evaluate the proposed *LeafNet* method qualitative performance based on class activation and localization. The findings are shown in Figure 5, which shows how well the *LeafNet* detects healthy and plagued regions inside complex input images. In addition, we included feature maps based on the activation and backbone maps of *LeafNet* for each and every test sample. These feature maps emphasize the most prominent elements of the given leaf image that the model found interesting. *LeafNet* highlights the localized areas using gradient-weighted class activation mapping (Grad-CAM) heat maps. Grad-CAM highlights the region of interest by presenting heat maps. The area that is more significant for decision-making in classification is depicted in red or orange, emphasizing the crucial features. Conversely, the colder regions are less prominent for the intended model. Figure 5 presents the visual results of the *LeafNet* framework for the most challenging examples that were taken randomly from the employed datasets. The input photos from the included datasets are represented by the first, sixth, eleventh, and sixteenth rows for each collection. The activation maps and core feature maps for each class are shown in the second and third rows. On the other hand, the final and second-to-last row shows the predicted label using *LeafNet* and the ground truth (GT).

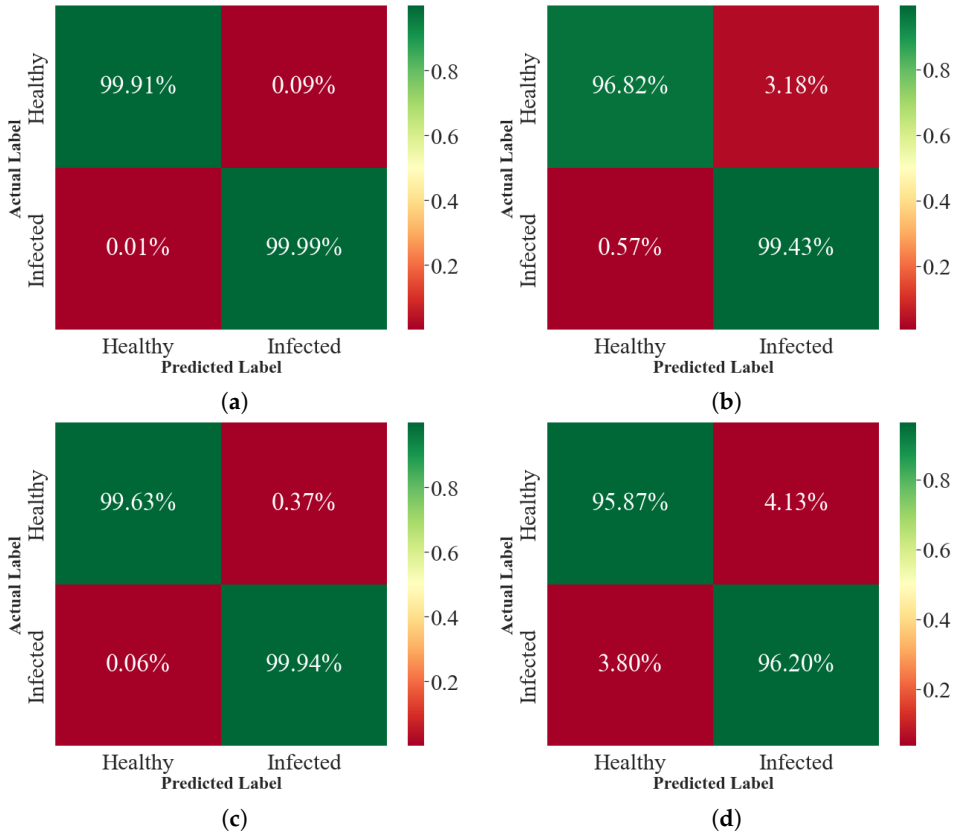

Figure 3. Confusion matrices of the proposed *LeafNet* for every dataset that is part of the experiment. (**a**) PV. (**b**) DRLI. (**c**) PC. (**d**) BARI-Sun.

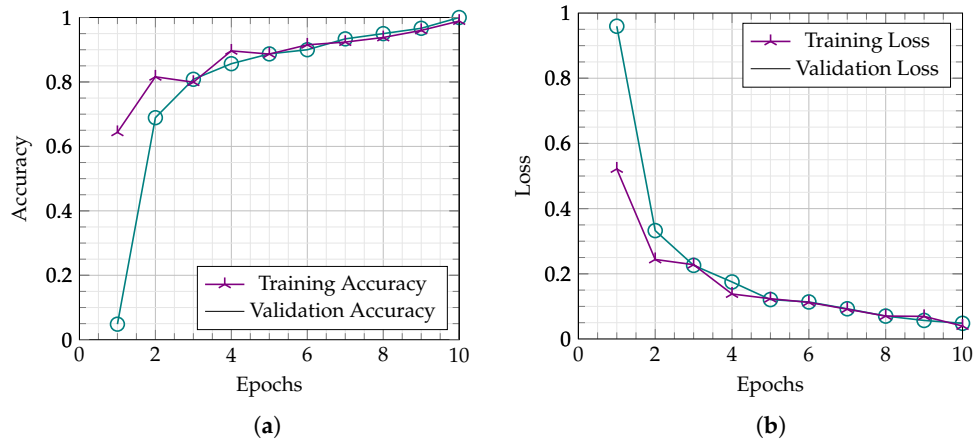

Figure 4. The accuracy and loss of the suggested *LeafNet* method during training and validation on the PC dataset. (**a**) Accuracy. (**b**) Loss.

The first, second and the third sets of input images, which are healthy and infected, respectively, were successfully labeled, and the last set of input images, which contains three infected leaf images and three healthy leaf images were misclassified altogether. In the three infected images, the model is not looking at the infected regions, which are too small and difficult to identify even by the naked eye; instead, *LeafNet* is focusing on the healthy parts of the leaf. On the contrary, for the three healthy images, *LeafNet* is mistakenly classifying the healthy input images as infected although the fourth and fifth images are depicting that leaves are healthy but there are some similarities that match and look like powdery mildew infection due to which the model is misclassifying the targeted image.

The last healthy is quite deceptive for *LeafNet* due to its small size and low number of such samples in the dataset.

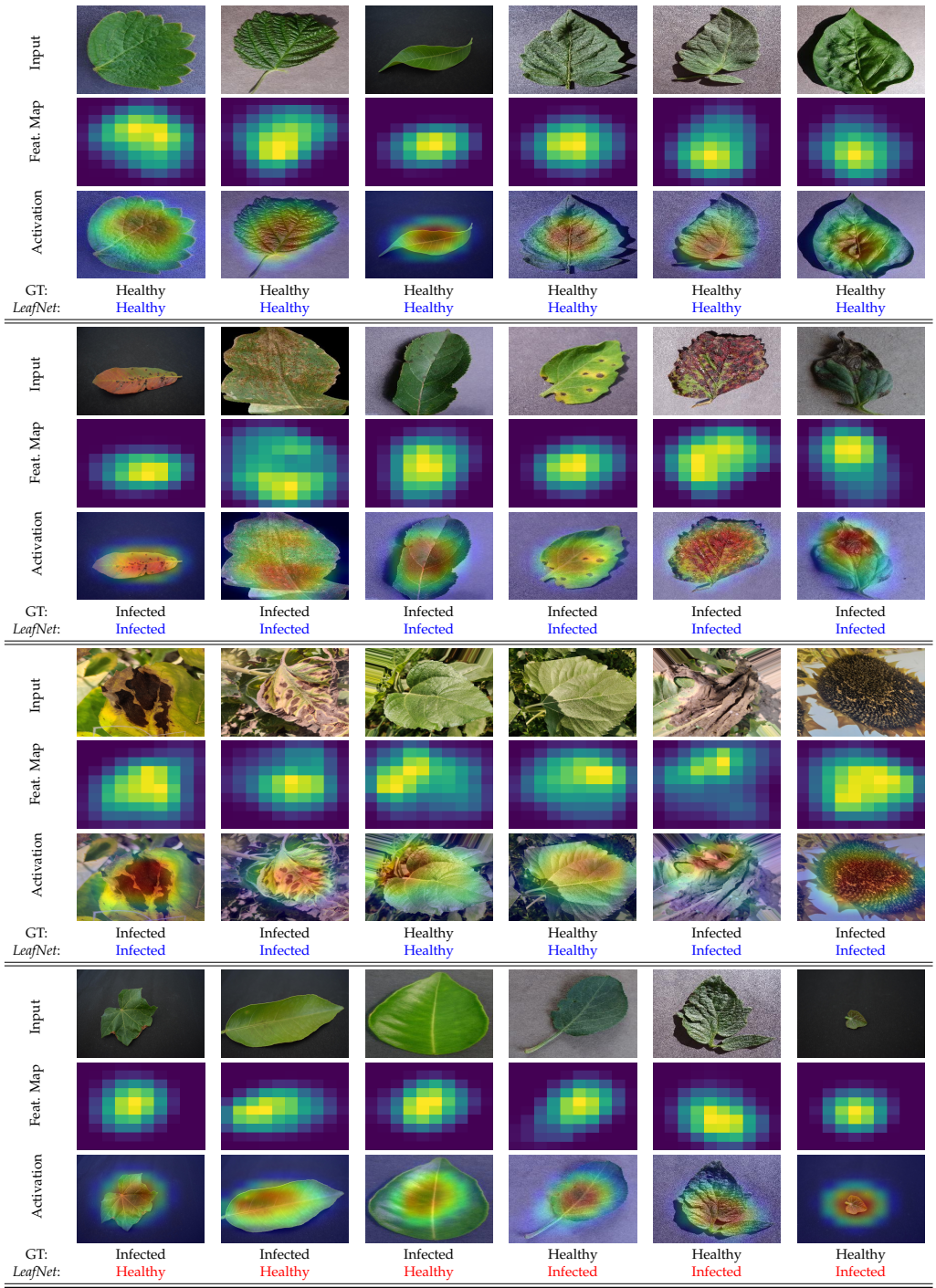

Figure 5. Qualitative evaluation of *LeafNet* using the included datasets. Results for the accurate prediction of the input images are highlighted in blue, while the red represents the inaccurate.

4.6. Time Complexity Analysis

A real-time assessment on a variety of devices is essential to credibly evaluate the efficacy, performance, and deployment suitability of a DL model. One such device is the Raspberry Pi 4 (Model B+), a small edge device with a quad-core Cortex-A72 64-bit processor running at 1.5 GHz and 4 GB of RAM. Section 4.1 contains comprehensive CPU specs and a frame-per-second (FPS) analysis for the suggested *LeafNet*. An FPS of 30 or more is the standard for evaluating the model's performance in ideal applications since

this is considered appropriate for real-world settings [47]. We used a plant disease video from an online source in order to grade the model's performance. Using the RPi 4B+ and the system CPU, our suggested *LeafNet* model yielded FPS values of 8.67 and 25.84, respectively. The closest to the *LeafNet* in terms of FPS and model size were MobileNetV1 and MobileOne-S; however, the proposed method performs better with low size on the disk as 4.40 megabyte (MB), less number of trainable parameters and FLOPs, i.e., 1.14 million and 157 million, respectively. The suggested *LeafNet* model's FPS performance is contrasted with other baseline models in Table 4.

Table 4. A comparison of the *LeafNet* FPS with a number of other DL techniques. The comparative inference speed performance of each model is provided, where the blue color highlights the *LeafNet* model. Smaller values are better, as shown by the downward arrow (⇓), and higher values are better, as indicated by the upward arrow (⇑).

Technique	Parameters (M) ⇓	Size (MB) ⇓	FLOPs (M) ⇓	FPS ⇑	
				RPi 4B+	CPU
VGG19	143.7	549.0	19,630	0.47	9.49
VGG16	138.4	528.0	15,500	0.62	11.09
EfficientNetB0	5.3	29.0	390	2.69	19.74
MobileNetV1	4.3	16.0	300	8.23	22.96
MobileNetV3Small	2.9	18.0	19.42	7.43	27.94
ResNet50	25.6	98.0	3800	4.30	19.83
ResNet152	60.4	232.0	11,000	0.39	15.43
ViT-B/32	86.0	345.0	8650	0.21	19.83
MobileViT-S	5.6	22.0	1792	2.47	17.46
MobileOne-S0	2.1	3.0	275	8.15	26.89
The proposed *LeafNet*	1.14	4.40	157	8.67	25.84

4.7. Discussion

This study underscores the importance of early plant disease detection for agricultural sustainability and introduces *LeafNet* as a lightweight, efficient solution designed for resource-constrained environments. By significantly reducing the model size from 143 M to 1.14 M parameters while maintaining competitive accuracy, *LeafNet* bridges the gap between high-performance DL and real-world applicability. The model's integration of channel attention mechanisms enhances its ability to focus on disease-relevant features, validated through experiments on four datasets: PV, DRLI, PC, and the BARI-Sun dataset. Robust accuracies of 0.99%, 0.98%, 0.99%, and 0.96% demonstrate *LeafNet*'s adaptability to diverse indoor and outdoor conditions. In comparison to other lightweight models such as MobileOne-S0 and MobileNetV3Small, *LeafNet* offers a unique trade-off between model size, computational efficiency, and accuracy. For example, while MobileOne-S0 achieves a comparable FPS of 8.15 on RPi 4B+, *LeafNet* outperforms it slightly at 8.67 FPS while maintaining fewer parameters (1.14 M vs. 2.1 M) and lower FLOPs (157 M vs. 275 M). This highlights *LeafNet*'s efficiency, particularly in scenarios requiring real-time disease detection on edge devices. The resultant FPS of 8.67 on RPi 4B+ is adequate for real-time applications, supported by references [47–51] indicating similar benchmarks in real-world use cases. However, certain limitations remain. The current implementation focuses on a limited range of crops and diseases, and further research should extend its applicability to more diverse datasets. Additionally, the model's performance could benefit from testing in varied, uncontrolled environments to better simulate real-world agricultural settings.

Potential applications for *LeafNet* include integration with IoT systems for automated disease monitoring and precise data collection, paving the way for predictive analytics

in smart farming. Exploring advanced attention mechanisms could also enhance its feature extraction capabilities, making it even more robust in challenging scenarios such as occluded or damaged leaves. In summary, *LeafNet* delivers a compelling combination of accuracy, efficiency, and scalability, establishing itself as a transformative tool for precision agriculture. Its readiness for deployment and potential to support sustainable farming practices make it a valuable contribution to modern agricultural technology.

5. Conclusions

This study claims to present an improved VGG19-based approach for detecting plant diseases and infections that outperforms current state-of-the-art research. In addition, the suggested *LeafNet* was altered to reduce the number of parameters from 143 M to 1.14 M in order to improve the method's performance. Four datasets in total—the PC, DRLI, PV and BARI-Sun—were used to assess the proposed *LeafNet*. In order to demonstrate the model's capacity for applicability in practical contexts, the research also presents extensive quantitative and qualitative studies. Using an edge device, such as RPi 4B+, the proposed *LeafNet* was tested for FPS. **Limitations and Future Work:** The proposed *LeafNet* has some limitations, as evidenced by the qualitative study, where it misclassified certain samples. These limitations primarily stem from factors such as the small number of instances, low-resolution images, and, in some cases, insufficient focus on small infected areas. To address these challenges, future work could explore incorporating self-attention and cross-attention mechanisms. These approaches have the potential to enhance feature extraction by better capturing relevant details, particularly in scenarios involving subtle or localized infections. In the context of intelligent edge devices, leveraging these advanced attention-based models offers a promising avenue for further research and improvement.

Author Contributions: Methodology, software, validation, S.P. and N.D.; formal analysis, N.D. and J.W.L.; investigation, N.D.; resources, J.W.L.; writing—original draft, S.P.; writing—review & editing, N.D. and J.W.L.; visualization, N.D.; supervision, J.W.L.; project administration, J.W.L.; funding acquisition, J.W.L. S.P. and N.D. contributed equally to this work and are co-first authors. All authors have read and agreed to the published version of the'manuscript.

Funding: This research was supported by the MSIT (Ministry of Science and ICT), South Korea, under the ITRC (Information Technology Research Center) support program (IITP-2024-RS-2022-00156354) supervised by the IITP (Institute for Information & Communications Technology Planning & Evaluation). It was also supported by the Institute of Information and Communications Technology Planning and Evaluation (IITP) under the metaverse support program to nurture the best talents (IITP-2023-RS-2023-00254529) grant funded by the Korean Government (MSIT).

Institutional Review Board Statement: Not applicable.

Data Availability Statement: The datasets utilized in this study are openly available at PV Dataset (https://github.com/spMohanty/PlantVillage-Dataset) (accessed on 5 January 2024), DRLI Dataset (https://data.mendeley.com/datasets/hb74ynkjcn/1) (accessed on 5 January 2024) and BARI-Sun Dataset (https://data.mendeley.com/datasets/b83hmrzth8/1) (accessed on 5 January 2024).

Conflicts of Interest: The authors declare no conflict of interest.

References

1. Bank, W. World Bank Survey. 2021. Available online: https://data.worldbank.org/indicator/SL.AGR.EMPL.ZS (accessed on 5 June 2023).
2. Clock, W.F. World Food Clock. 2014. Available online: http://worldfoodclock.com/ (accessed on 5 June 2023).
3. Thilagavathi, M.; Abirami, S. Application of image processing in diagnosing guava leaf diseases. *Int. J. Sci. Res. Manag.* **2017**, *5*, 5927–5933.

4. Gavhale, K.R.; Gawande, U.; Hajari, K.O. Unhealthy region of citrus leaf detection using image processing techniques. In Proceedings of the International Conference for Convergence for Technology—2014, Pune, India, 6–8 April 2014; IEEE: Piscataway, NJ, USA, 2014; pp. 1–6.
5. Padol, P.B.; Yadav, A.A. SVM classifier based grape leaf disease detection. In Proceedings of the 2016 Conference on Advances in Signal Processing (CASP), Pune, India, 9–11 June 2016; IEEE: Piscataway, NJ, USA, 2016; pp. 175–179.
6. Masazhar, A.N.I.; Kamal, M.M. Digital image processing technique for palm oil leaf disease detection using multiclass SVM classifier. In Proceedings of the 2017 IEEE 4th International Conference on Smart Instrumentation, Measurement and Application (ICSIMA), Putrajaya, Malaysia, 28–30 November 2017; IEEE: Piscataway, NJ, USA, 2017; pp. 1–6.
7. Islam, M.; Dinh, A.; Wahid, K.; Bhowmik, P. Detection of potato diseases using image segmentation and multiclass support vector machine. In Proceedings of the 2017 IEEE 30th Canadian Conference on Electrical and Computer Engineering (CCECE), Windsor, ON, Canada, 30 April–3 May 2017; IEEE: Piscataway, NJ, USA, 2017; pp. 1–4.
8. Agrawal, N.; Singhai, J.; Agarwal, D.K. Grape leaf disease detection and classification using multi-class support vector machine. In Proceedings of the 2017 International Conference on Recent Innovations in Signal Processing and Embedded Systems (RISE), Bhopal, India, 27–29 October 2017; IEEE: Piscataway, NJ, USA, 2017; pp. 238–244.
9. Parikh, A.; Raval, M.S.; Parmar, C.; Chaudhary, S. Disease detection and severity estimation in cotton plant from unconstrained images. In Proceedings of the 2016 IEEE International Conference on Data Science and Advanced Analytics (DSAA), Montreal, QC, Canada, 17–19 October 2016; IEEE: Piscataway, NJ, USA, 2016; pp. 594–601.
10. Suresha, M.; Shreekanth, K.; Thirumalesh, B. Recognition of diseases in paddy leaves using knn classifier. In Proceedings of the 2017 2nd International Conference for Convergence in Technology (I2CT), Mumbai, India, 7–9 April 2017; IEEE: Piscataway, NJ, USA, 2017; pp. 663–666.
11. Vaishnnave, M.; Devi, K.S.; Srinivasan, P.; Jothi, G.A.P. Detection and classification of groundnut leaf diseases using KNN classifier. In Proceedings of the 2019 IEEE International Conference on System, Computation, Automation and Networking (ICSCAN), Pondicherry, India, 29–30 March 2019; IEEE: Piscataway, NJ, USA, 2019; pp. 1–5.
12. Liu, H.; Lang, B. Machine learning and deep learning methods for intrusion detection systems: A survey. *Appl. Sci.* **2019**, *9*, 4396. [CrossRef]
13. Mohanty, S.P.; Hughes, D.P.; Salathé, M. Using deep learning for image-based plant disease detection. *Front. Plant Sci.* **2016**, *7*, 1419. [CrossRef] [PubMed]
14. Chouhan, S.S.; Singh, U.P.; Kaul, A.; Jain, S. A data repository of leaf images: Practice towards plant conservation with plant pathology. In Proceedings of the 2019 4th International Conference on Information Systems and Computer Networks (ISCON), Mathura, India, 21–22 November 2019; IEEE: Piscataway, NJ, USA, 2019; pp. 700–707.
15. Dhaka, V.S.; Meena, S.V.; Rani, G.; Sinwar, D.; Ijaz, M.F.; Woźniak, M. A survey of deep convolutional neural networks applied for prediction of plant leaf diseases. *Sensors* **2021**, *21*, 4749. [CrossRef] [PubMed]
16. Qiu, R.; Yang, C.; Moghimi, A.; Zhang, M.; Steffenson, B.J.; Hirsch, C.D. Detection of fusarium head blight in wheat using a deep neural network and color imaging. *Remote Sens.* **2019**, *11*, 2658. [CrossRef]
17. Bi, C.; Wang, J.; Duan, Y.; Fu, B.; Kang, J.R.; Shi, Y. MobileNet based apple leaf diseases identification. *Mob. Netw. Appl.* **2022**, *27*, 172–180. [CrossRef]
18. Lee, S.H.; Goëau, H.; Bonnet, P.; Joly, A. New perspectives on plant disease characterization based on deep learning. *Comput. Electron. Agric.* **2020**, *170*, 105220. [CrossRef]
19. Kundu, N.; Rani, G.; Dhaka, V.S.; Gupta, K.; Nayak, S.C.; Verma, S.; Ijaz, M.F.; Woźniak, M. IoT and interpretable machine learning based framework for disease prediction in pearl millet. *Sensors* **2021**, *21*, 5386. [CrossRef]
20. Rangarajan, A.K.; Purushothaman, R.; Ramesh, A. Tomato crop disease classification using pre-trained deep learning algorithm. *Procedia Comput. Sci.* **2018**, *133*, 1040–1047. [CrossRef]
21. Amara, J.; Bouaziz, B.; Algergawy, A. A deep learning-based approach for banana leaf diseases classification. In *Datenbanksysteme für Business, Technologie und Web (BTW 2017)-Workshopband*; German Informatics Society: Bonn, Germany, 2017.
22. Barbedo, J.G.A. A review on the use of unmanned aerial vehicles and imaging sensors for monitoring and assessing plant stresses. *Drones* **2019**, *3*, 40. [CrossRef]
23. Simonyan, K.; Zisserman, A. Very deep convolutional networks for large-scale image recognition. *arXiv* **2014**, arXiv:1409.1556.
24. Tan, M.; Le, Q. Efficientnet: Rethinking model scaling for convolutional neural networks. In Proceedings of the International Conference on Machine Learning, PMLR, Long Beach, CA, USA, 9–15 June 2019; pp. 6105–6114.
25. Howard, A.G.; Zhu, M.; Chen, B.; Kalenichenko, D.; Wang, W.; Weyand, T.; Andreetto, M.; Adam, H. Mobilenets: Efficient convolutional neural networks for mobile vision applications. *arXiv* **2017**, arXiv:1704.04861.
26. Howard, A.; Sandler, M.; Chu, G.; Chen, L.C.; Chen, B.; Tan, M.; Wang, W.; Zhu, Y.; Pang, R.; Vasudevan, V.; et al. Searching for mobilenetv3. In Proceedings of the Proceedings of the IEEE/CVF International Conference on Computer Vision, Seoul, Republic of Korea, 27 October–2 November 2019; pp. 1314–1324.

27. He, K.; Zhang, X.; Ren, S.; Sun, J. Deep residual learning for image recognition. In Proceedings of the IEEE Conference on Computer Vision and Pattern Recognition, Las Vegas, NV, USA, 27–30 June 2016; pp. 770–778.
28. Dosovitskiy, A.; Beyer, L.; Kolesnikov, A.; Weissenborn, D.; Zhai, X.; Unterthiner, T.; Dehghani, M.; Minderer, M.; Heigold, G.; Gelly, S.; et al. An image is worth 16x16 words: Transformers for image recognition at scale. *arXiv* **2020**, arXiv:2010.11929.
29. Mehta, S.; Rastegari, M. Mobilevit: Light-weight, general-purpose, and mobile-friendly vision transformer. *arXiv* **2021**, arXiv:2110.02178.
30. Vasu, P.K.A.; Gabriel, J.; Zhu, J.; Tuzel, O.; Ranjan, A. Mobileone: An improved one millisecond mobile backbone. In Proceedings of the IEEE/CVF Conference on Computer Vision and Pattern Recognition, Vancouver, BC, Canada, 18–22 June 2023; pp. 7907–7917.
31. Zhao, Y.; Sun, C.; Xu, X.; Chen, J. RIC-Net: A plant disease classification model based on the fusion of Inception and residual structure and embedded attention mechanism. *Comput. Electron. Agric.* **2022**, *193*, 106644. [CrossRef]
32. Pandey, A.; Jain, K. A robust deep attention dense convolutional neural network for plant leaf disease identification and classification from smart phone captured real world images. *Ecol. Inform.* **2022**, *70*, 101725. [CrossRef]
33. Bedi, P.; Gole, P. Plant disease detection using hybrid model based on convolutional autoencoder and convolutional neural network. *Artif. Intell. Agric.* **2021**, *5*, 90–101. [CrossRef]
34. Chohan, M.; Khan, A.; Chohan, R.; Katpar, S.H.; Mahar, M.S. Plant disease detection using deep learning. *Int. J. Recent Technol. Eng.* **2020**, *9*, 909–914. [CrossRef]
35. Hassan, S.M.; Maji, A.K. Plant disease identification using a novel convolutional neural network. *IEEE Access* **2022**, *10*, 5390–5401. [CrossRef]
36. Atila, Ü.; Uçar, M.; Akyol, K.; Uçar, E. Plant leaf disease classification using EfficientNet deep learning model. *Ecol. Inform.* **2021**, *61*, 101182. [CrossRef]
37. Amin, H.; Darwish, A.; Hassanien, A.E.; Soliman, M. End-to-end deep learning model for corn leaf disease classification. *IEEE Access* **2022**, *10*, 31103–31115. [CrossRef]
38. Maurya, R.; Pandey, N.N.; Singh, V.P.; Gopalakrishnan, T. Plant disease classification using interpretable vision transformer network. In Proceedings of the 2023 International Conference on Recent Advances in Electrical, Electronics & Digital Healthcare Technologies (REEDCON), New Delhi, India, 1–3 May 2023; IEEE: Piscataway, NJ, USA, 2023, pp. 688–692.
39. Abbas, A.; Jain, S.; Gour, M.; Vankudothu, S. Tomato plant disease detection using transfer learning with C-GAN synthetic images. *Comput. Electron. Agric.* **2021**, *187*, 106279. [CrossRef]
40. Thakur, P.S.; Khanna, P.; Sheorey, T.; Ojha, A. Explainable vision transformer enabled convolutional neural network for plant disease identification: PlantXViT. *arXiv* **2022**, arXiv:2207.07919.
41. Karthik, R.; Hariharan, M.; Anand, S.; Mathikshara, P.; Johnson, A.; Menaka, R. Attention embedded residual CNN for disease detection in tomato leaves. *Appl. Soft Comput.* **2020**, *86*, 105933.
42. Dai, G.; Tian, Z.; Fan, J.; Sunil, C.; Dewi, C. DFN-PSAN: Multi-level deep information feature fusion extraction network for interpretable plant disease classification. *Comput. Electron. Agric.* **2024**, *216*, 108481. [CrossRef]
43. Shah, D.; Trivedi, V.; Sheth, V.; Shah, A.; Chauhan, U. ResTS: Residual deep interpretable architecture for plant disease detection. *Inf. Process. Agric.* **2022**, *9*, 212–223. [CrossRef]
44. Gupta, B.B.; Quamara, M. An overview of Internet of Things (IoT): Architectural aspects, challenges, and protocols. *Concurr. Comput. Pract. Exp.* **2020**, *32*, e4946. [CrossRef]
45. Keras. Keras Applications. 2024. Available online: https://keras.io/api/applications/ (accessed on 23 December 2024).
46. Sara, U.; Rajbongshi, A.; Shakil, R.; Akter, B.; Sazzad, S.; Uddin, M.S. An extensive sunflower dataset representation for successful identification and classification of sunflower diseases. *Data Brief* **2022**, *42*, 108043. [CrossRef] [PubMed]
47. Parez, S.; Dilshad, N.; Alghamdi, N.S.; Alanazi, T.M.; Lee, J.W. Visual intelligence in precision agriculture: Exploring plant disease detection via efficient vision transformers. *Sensors* **2023**, *23*, 6949. [CrossRef] [PubMed]
48. Parez, S.; Dilshad, N.; Alanazi, T.M.; Lee, J.W. Towards Sustainable Agricultural Systems: A Lightweight Deep Learning Model for Plant Disease Detection. *Comput. Syst. Sci. Eng.* **2023**, *47*, 515–536. [CrossRef]
49. Dilshad, N.; Khan, S.U.; Alghamdi, N.S.; Taleb, T.; Song, J. Towards efficient fire detection in IoT environment: A modified attention network and large-scale dataset. *IEEE Internet Things J.* **2023**, *11*, 13467–13481. [CrossRef]
50. Dilshad, N.; Khan, T.; Song, J. Efficient Deep Learning Framework for Fire Detection in Complex Surveillance Environment. *Comput. Syst. Sci. Eng.* **2023**, *46*, 749–764. [CrossRef]
51. Khan, Z.A.; Ullah, F.U.M.; Yar, H.; Ullah, W.; Khan, N.; Kim, M.J.; Baik, S.W. Optimized Cross-Module Attention Network and Medium-Scale Dataset for Effective Fire Detection. *Pattern Recognit.* **2024**, *161*, 111273. [CrossRef]